217

OPTICAL MEASUREMENT OF NUMBER DENSITY, ABSORPTION COEFFICIENT, AND INDEX OF REFRACTION OF DILUTE SODIUM VAPOR

A thesis submitted to the

School of Graduate Studies

Addis Ababa University

In partial fulfillment

of the requirements for the degree

of Masters of Science in Physics

By

Tulu Benti Bacha

June 2001

ADDIS ABABA UNIVERSITY

Addis Ababa University

Abstract

OPTICAL MEASUREMENT OF NUMBER DENSITY, ABSORPTION COEFFICIENT, AND INDEX OF REFRACTION OF DILUTE SODIUM VAPOR

By: Tulu Benti Bacha

In this thesis, the number density and vapor pressure of a sodium atom in the temperature ranges 337 K, close to room temperature, up to 511 K are determined from the measurement of the transmittance and temperature of the sample. The broadening parameters at different temperatures are determined for the two lines. The absorption coefficients, and index of refraction of the sodium atom in the optical region, at the D lines (589.76 nm and 589.16 nm), are obtained.

TABLE OF CONTENTS

LIST OF FIGURES

Number *Page*

ACKNOWLEDGMENTS

I would like to express my deepest gratitude to my advisor, Dr. Araya A., for his invaluable advise, guidance and encouragement during my work. Secondly, I would like to express my indebtedness to the ICTP for their financial support. In addition, my sincere thanks go to the Physics Department Staff Members, in general, to my instructors, in particular.

Finally, I would like to express my deep gratitude to my parents for their encouragements during my entire educational journey

Chapter 1

INTRODUCTION

All alkali metals have been the focus of substantial theoretical and experimental efforts for some time. They form one group, in which theory and experiment can be compared most favorably since they present a simple system with only one electron outside of a closed shell, therefore approximating a hydrogenic system. For instance, Ditchburn and Opik [1] summarized the results obtained for the continuous absorption cross-section of the alkali metals and conclude that the agreement between theory and experiment is good for photon energies up to about 4.836×10^{14} Hz above the ionization limit. In particular, Hudson [2] measured the continuous absorption cross-section of atomic sodium in the wavelength range between 240 nm and 100 nm.

Atomic absorption is widely applied in astrophysics, medical, agricultural and industrial fields for determination of trace concentration of elements. Knowledge of the atomic number densities in the ground levels is essential for the interpretation of data in atomic physics experiments. The required number densities can be obtained by measuring the absorption of the vapor when illuminated by light of the resonance or other suitable line. This is particularly true

for the alkali metals where optical pumping experiments are frequently used. In this thesis, with the optical method, accurate measurement of transmission is carried out from which the atomic number density is determined. From the knowledge of the atomic number density one can determine the pressure of the vapor. Conventionally, sensitive devices are needed to measure the pressure of a diluted vapor near room temperatures. However, once the atomic number densities in the vapor are obtained by optical means the corresponding vapor pressures can also be determined accurately. Bjorkholm and Ashkin [3] measured the number density of sodium at 453 K and 473 K. JANAF [4], Hultger et al [5], Honig [6], and Nesmeynov [7] reported vapor pressure of sodium in the temperature ranges of 600 K and 900 K. Nevertheless, the vapor pressure of sodium below 450 K has never been measured. In this thesis, it is shown that the pressure obtained in the temperature ranges 337 K, which is close to the room temperature and up to 511 K with the optical method along with modeling of the spectral lines with the method developed by Asfaw [4] ranges from 76 $nTorr$ to 8 $\mu Torr$.

This thesis has four chapters. The second chapter focuses mainly on the theoretical background, which deals with the phenomenological explanation of interaction of radiation with a gaseous medium and effects of collision and motion of atoms of the medium on the observed line profiles. The third part deals with the experimental works and the analysis of the data. From the measured quantities, transmittance and temperature, with the appropriate modeling of the line profile

the atomic number density, the vapor pressure, the absorption cross-sections and the real part of the complex index of refraction are plotted. In addition, the broadening parameters are obtained at different temperatures. The pressure broadening parameters at sodium D transitions ($3s_{1/2} - 3p_{3/2}$ and $3s_{1/2} - 3p_{1/2}$) are determined using the Voigt profile for the expression in the absorption cross-sections. Moreover, in this low-pressure ranges and the corresponding temperatures the feature of the real part of the complex index of refraction versus frequency is plotted for each line separately. The real part of the complex index of refraction is expressed in terms of the imaginary part of the complex probability function $w(z)$. With the knowledge of the broadening parameters and the number density, the profile of the index of refraction near resonance line is plotted. The sodium metal is heated up with infrared radiator. The power of the infrared radiator is controlled by a variac and a sodium lamp is used to illuminate the sample.

The spectrometer used in this experiment has a resolution of about 0.25 nm at 590 nm. In the last chapter, the main results of the work is discussed shortly.

Chapter 2

THE CLASSICAL THEORY OF ABSORPTION AND PHENOMENOLOGICAL DESCRIPTION OF DISPERSION OF ELECTROMAGNETIC RADIATION IN A MEDIUM

The physics of absorption process is simplest in well-isolated atoms. These are found most commonly in gases. White light propagating through a gas is absorbed at resonance frequencies of the atoms so that one observes gaps in the wavelength distribution of the emerging light. Most atoms have electronic resonance frequencies in the ultraviolet, although resonance in the visible and infrared region is also common. For instance, atomic sodium has strong absorption lines in the yellow region at 589.76 nm and 589.16 nm. The electronic resonance in molecules also tends to lie in the ultraviolet. We have white daylight because the atmosphere, mostly consists of N_2 and O_2, does not absorb strongly at visible frequencies.

We observe the effects of interaction of radiation with matter such as absorption and dispersion. The theoretical analysis that relates these macroscopic effects to the microscopic properties of the material is the Lorentz theory of dispersion [9, 10]. In view of this theory absorption and dispersion are two manifestations of the same physical process.

According to Lorentz's theory, the medium in which the electromagnetic radiation propagates is considered as a collection of dipoles that are driven by the radiation. The electromagnetic radiation interacting with a polarizable medium induces in the individual atom or molecule an electric dipole moment $\vec{p}$, which is given as [9]

$$\vec{p} = \alpha \vec{E}(\vec{x},t) \tag{1}$$

where α is the polarizability of the medium, and $\vec{E}(\vec{x},t)$ is the electric field. In a homogeneous medium, the induced dipole moments form a macroscopic polarization $\vec{P}$, which is the sum of all dipole moments per unit volume, is given by [9]

$$\vec{P} = n\alpha \vec{E}(\vec{x},t) \tag{2}$$

where n is the atomic number density in the medium. The Lorentz theory asserted that the electron in unclosed shell of an atom, under the influence of electromagnetic radiation field, experiences the Lorentz force and is displaced from its unperturbed position. The equation of motion of an electron of charge $-e$ bound to the atom acted on by electromagnetic radiation is [9]

$$m\left(\frac{d^2\vec{x}}{dt^2} + \gamma \frac{d\vec{x}}{dt} + {\omega_0}^2 \vec{x}\right) = -e\vec{E}(\vec{x},t) \tag{3}$$

where γ measures the phenomenological damping force constant, m is the mass of electron and ω_0 the angular frequency of oscillation of the electron bound to the atom [11]. With the approximation that the amplitude of oscillation is small, we can assume that the local electric field at average position of the electron to be the externally applied radiation field. When the field varies harmonically in time with angular frequency ω, as $e^{i\omega t}$, the dipole moment contributed by one electron of an atom, with oscillator strength f, is given as [11]:

$$\vec{p} = -e\vec{x} = -\frac{e^2 f}{m}\left(\omega_0{}^2 - \omega^2 - i\gamma\omega\right)^{-1}\vec{E}(\vec{x},t)\,. \tag{4}$$

If there are n atoms per unit volume each with q valence electrons having oscillation frequency ω_i and damping constant γ_i, then the polarization density of the medium is:

$$\vec{P} = -e\vec{x} = -\frac{ne^2}{m}\sum_{i=1}^{q} f_i\left(\omega_0{}^2 - \omega_i{}^2 - i\gamma_i\omega_i\right)^{-1}\vec{E}(\vec{x},t) \tag{5}$$

where f_i is the oscillator strength satisfying the sum rule $\sum f_i = q$ [12]. Up on comparing the above equations we have an expression for the polarizability as:

$$\alpha(\omega) = \frac{e^2}{m}\sum_{i=1}^{q} f_i\left(\omega_i{}^2 - \omega^2 - i\gamma_i\omega\right)^{-1} \tag{6}$$

With suitable quantum mechanical definitions of f_i, γ_i, ω_i the above equation is an accurate description for the atomic polarization density. In the following section we will see the features of the line profile of the alkali metals for which q is one.

Widths and Profiles of Spectral Lines

Spectral lines of absorbing or emitting atoms can give us important information about the atoms. In particular, the shape and the width of the spectral lines can provide us the information we seek.

In discrete absorption or emission spectra, spectral lines are not strictly monochromatic. The profile of every spectral line has a finite width and characteristic shape. We observe spectral distribution $I(\nu)$ of an absorbed or an emitted intensity near the central frequency ν_0. In other words, the spectral lines are broadened. The broadening of the spectral lines can be pressure or Doppler or both. A radiation is strongly absorbed when it is nearly at resonance with one of the natural oscillation frequencies of the absorbing atoms. This absorption can be explained by the assumption that the Lorentz electron oscillators are subject to a damping force that arises naturally as a result of collision [11].

Under most circumstances in gaseous media the broadening of spectral lines is due mainly to collisions (pressure broadening) and atomic motion (Doppler

broadening). However, a spectral line would still have a non-vanishing natural line width.

Natural Broadening

An excited atom can emit its excitation energy as spontaneous radiation. In order to investigate the spectral distribution of the spontaneous emission on a transition we shall describe the excited atomic electron by the classical model of a damped harmonic oscillator with frequency ω, mass m, restoring force constant k and the damping constant γ_n. The amplitude $\vec{x}(t)$ of oscillation can be obtained by solving the differential equation of motion of the bound electron [13]:

$$\frac{d^2\vec{x}}{dt^2} + \gamma_n \frac{d\vec{x}}{dt} + \omega_0{}^2 \vec{x} = 0 \tag{7}$$

where $\omega_0 = \sqrt{\frac{k}{m}}$. With the initial conditions $\vec{x}(0) = \vec{x}_0$ and $\frac{d\vec{x}(0)}{dt} = 0$, the real solution is

$$\vec{x}(t) = \vec{x}_0 e^{-\frac{\gamma_n}{2}t} (\cos\omega_0 t + \frac{\gamma_n}{2\omega_0} \sin\omega_0 t). \tag{8}$$

However, for small damping the solution reduces to

$$\vec{x}(t) = \vec{x}_0 e^{-\frac{\gamma_n}{2}t} \cos\omega_0 t \tag{9}$$

The oscillation $\vec{x}(t)$ can be described as a superposition of harmonic oscillations $e^{i\omega t}$ with amplitude $\vec{A}(\omega)$ [13]

$$\vec{x}(t) = \frac{1}{\sqrt{2\pi}} \int_{\infty}^{+\infty} \vec{A}(\omega) e^{i\omega t} d\omega \,. \tag{10}$$

By Fourier transformation we can obtain $\vec{A}(\omega)$ as

$$\begin{aligned}
\vec{A}(\omega) &= \frac{1}{\sqrt{2\pi}} \int_{0}^{+\infty} \vec{x}(t) e^{-i\omega t} dt \\
&= \frac{1}{\sqrt{2\pi}} \int_{0}^{+\infty} \vec{x}_0 e^{-\frac{\gamma_n}{2}t} \cos\omega_0 t \cdot e^{-i\omega t} dt \\
&= \frac{1}{\sqrt{2\pi}} \frac{\vec{x}_0}{2} \int_{0}^{\infty} \left(e^{i(\omega_0-\omega)t - i\frac{\gamma_n}{2}t}{}_n + e^{i(\omega_0+\omega)t + i\frac{\gamma_n}{2}t} \right) dt \\
&= \frac{\vec{x}_0}{2\sqrt{2\pi}} \left[\frac{1}{i(\omega-\omega_0) + \frac{\gamma_n}{2}} + \frac{1}{i(\omega+\omega_0) + \frac{\gamma_n}{2}} \right]
\end{aligned}$$

Since the term on the right hand side is significant only for frequencies ω near to the resonance frequency ω_0 of an atomic transition the second term is negligible. The intensity $I(\omega)$ of the profile of the spectral line is [13]

$$I(\omega) = \vec{A}(\omega) \bullet \vec{A}(\omega) = I_0 \frac{\gamma_n / 2\pi}{(\omega - \omega_0)^2 + \frac{\gamma_n^{\,2}}{4}} \tag{11}$$

This intensity distribution function is known as Lorentzian function. therefore, this line shape describes the natural width.

Relation between line width and lifetime

Recall the equation of motion of electron bound an atom

$$\frac{d^2\vec{x}}{dt^2} + \gamma_n \frac{d\vec{x}}{dt} + \omega_0^{\,2}\vec{x} = 0 \tag{12}$$

Multiplying by $m\frac{d\vec{x}}{dt}$ we obtain the radiant power of the damped oscillator as

$$m\frac{d^2\vec{x}}{dt^2}\left(\frac{d\vec{x}}{dt}\right) + m\omega_0^{\,2}\vec{x}\frac{d\vec{x}}{dt} = -m\gamma_n m\left(\frac{d\vec{x}}{dt}\right)^2$$

$$\frac{d}{dt}\left[\frac{m}{2}\left(\frac{d\vec{x}}{dt}\right)^2 + \frac{m}{2}\omega_0^{\,2}\vec{x}^2\right] = -m\gamma_n m\left(\frac{d\vec{x}}{dt}\right)^2$$

$$\frac{dW}{dt} = -m\gamma_n m\left(\frac{d\vec{x}}{dt}\right)^2 \cong \frac{\gamma_n \omega_0 m x_0^{\,2}}{2} e^{-\gamma_n t}$$

We can see that the time averaged radiant power decreases to $\frac{1}{e}$ of its initial value $I(0)$ after the decay time $\tau_i = \frac{1}{\gamma_n}$. The mean lifetime τ_i of an atomic level, say E_i, which decays exponentially by spontaneous emission, is related to the Einstein coefficient A_i as $\tau_i = \frac{1}{A_i}$ [11]. As a result, the natural HWHM (Half Width at Half Maximum) of the spectral line spontaneously emitted from the level E_i is $\delta\nu = \frac{A_i}{4\pi}$ in Hz. The finiteness of the lifetime of excited atoms results for the finiteness of the natural line width.

Natural Line Width of Absorbing Transition

The intensity of plane wave passing in z-direction through an absorbing sample decreases along the distance dz and is given by [13]

$$dI = -a_{ik} I dz \tag{13}$$

The absorption coefficient $a_{ik}(\omega)$ [cm^{-1}] for a transition $|i\rangle \rightarrow |k\rangle$ depends on the population densities n_i, n_k of the lower and the upper levels, respectively, and on the absorption cross-section σ_{ik} [cm^2] of each absorbing atom [13]:

$$a_{ik}(\omega) = \sigma_{ik}(\omega)\left[n \; - \frac{g_i}{g_k} n_k \right] \tag{14}$$

where g_i and g_k are the degeneracy of the lower and the upper levels, respectively. For sufficiently small intensities [$I(\omega)$] the induced absorption rate is small compared to the refilling rate of level $|i\rangle$ and the population density n_i does not depend on the intensity, $I(\omega)$. The absorption in such medium is linear absorption [13]. Thus $a_{ik}(\omega)$ reduces to $a_{ik}(\omega) = \sigma_{ik}(\omega) n_i$; and the intensity of the propagating wave in the absorbing medium is

$$I(\omega) = I_0 e^{-a_{ik}(\omega) z} \tag{15}$$

From this we see, that the incident intensity is attenuated by $e^{-a_{ik}(\omega)z}$. In order to determine $a_{ik}(\omega)$, we consider the electron as a classical oscillator under the influence of a driving force, $e\vec{E}(\vec{x},t)$ driven by the optical radiation field, $\vec{E}(\vec{x},t) = \vec{E}_0 e^{i\omega t}$. The corresponding differential equation of motion of the atomic electron has the solution

$$\vec{x}(t) = -\frac{e\vec{E}(\vec{x},t)}{m({\omega_0}^2 - \omega^2 - i\gamma_n \omega)}. \tag{16}$$

The forced oscillation of charge $-e$ generates an induced dipole moment

$$\vec{p} = -e\vec{x} = -\frac{e^2}{m}(\omega_0{}^2 - \omega^2 - i\gamma_n\omega)^{-1}\vec{E}(\vec{x},t) \tag{17}$$

In the sample with n oscillators per unit volume, the macroscopic polarization, which is the sum of all dipole moments per unit volume, is

$$\vec{P} = -ne\vec{x} = -\frac{e^2 n f_i}{m}(\omega_0{}^2 - \omega^2 - i\gamma_n\omega)^{-1}\vec{E}(\vec{x},t) \tag{18}$$

On the other hand, the polarization can be derived from Maxwell's equations using dielectric constant ε_0 or susceptibility χ [12]:

$$\vec{P} = \varepsilon_0(\varepsilon - 1)\vec{E}(\vec{x},t) = \varepsilon_0\chi\vec{E}(\vec{x},t) \tag{19}$$

Finally, from the above two equations one can obtain

$$n'^2 - 1 = \frac{ne^2 f_i}{m\varepsilon_0}\frac{1}{\omega_0{}^2 - \omega^2 - i\gamma_n\omega} \tag{20}$$

where $n' = \sqrt{\varepsilon}$ is the complex index of refraction [13], ε is the relative dielectric constant. For dilute gaseous or vapor media, this reduces to

$$n'-1=\frac{ne^2 f_i}{2m\varepsilon_0}\frac{1}{{\omega_0}^2-\omega^2-i\gamma_n\omega}=n'_R+in'_I \tag{21}$$

An electromagnetic radiation field $\vec{E}(\vec{x},t)=\vec{E}_0 e^{-i(\omega t-\vec{k}\bullet\vec{x})}$ passing through a medium with refractive index n' has the same frequency $\omega_n=\omega$ as in vacuum but a different wavevector $\vec{k}_n=n'\vec{k}=\vec{k}(n'_R+in'_I)$. Thus, one can see that the imaginary part of the complex refractive index n' is related to the absorption of the radiation, while the real part represents the dispersion of the wave. Here, n'_R and n'_I are the real and imaginary part of the complex index of refraction, respectively. The real part of the complex index of refraction is given as

$$n'_R(\omega)=1+\frac{ne^2 f}{2m\varepsilon_0}\frac{{\omega_0}^2-\omega^2}{({\omega_0}^2-\omega^2)^2+(\gamma_n\omega)^2} \tag{22}$$

The intensity $I(\omega)\propto\vec{E}\bullet\vec{E}$ decreases, with the assumption that $\vec{x}=(0,0,z)$, as

$$I(\omega)=I_0 e^{-2k_0 n'_I z} \tag{23}$$

from which we get

$$a(\omega) = \frac{2\omega_{0n'_I}}{c} = \frac{ne^2 f\omega_0}{m\varepsilon_0 c} \frac{\gamma_n \omega}{(\omega_0{}^2 - \omega^2)^2 + (\frac{\gamma_n \omega}{2})^2} \tag{24}$$

From this expression, we see that the absorption coefficient is proportional to the imaginary part of the complex index of refraction. Equations (22) and (24) are special cases of the Kramer's-Kronig dispersion relations [11, 12]. In the neighborhood of the atomic transitions they reduces to

$$n'_R(\omega) = 1 + \frac{ne^2 f}{4m\varepsilon_0\omega_0} \frac{\omega_0 - \omega}{(\omega_0 - \omega)^2 + (\frac{\gamma_n}{2})^2} \tag{25}$$

and

$$a(\omega) = \frac{ne^2 f\omega_0}{4m\varepsilon_0 c} \frac{\gamma_n}{(\omega_0 - \omega)^2 + (\frac{\gamma_n}{2})^2} \tag{26}$$

The absorption profile $a(\omega)$ is Lorentzian with FWHM of $\Delta\omega = \gamma_n$ which equals the natural line width. The above relations are valid for oscillators at rest in the observer's coordinate system. The thermal motion of the gaseous atoms introduces an additional broadening of the line profile, the Doppler broadening. Moreover,

there is also collisional interaction among and between the atoms in the vapor that contributes to the collision or pressure broadening.

Collision Broadening

When atom 1 with energy levels E_i and E_k approaches another atom 2, their energy level is shifted because of the interaction between them. This shift depends on the electron configuration and the distance between them. This mutual interaction is said to be collision interaction. As a result of this collision there is line broadening of the spectral line. The line broadening associated with collisions is homogeneous. This is because each atom can absorb radiation over a range of frequencies, due to interruptions of its dipole oscillations by collisions. Since the collsional history of every atom is assumed to be the same, no greater broadening is associated with a collection of atoms than is associated with individual atom. The line shape function associated with the collision broadening is described by a Lorenzian function.

Including additional damping constant, to that of the natural line, due to collisions, we consider these effects on the line profiles by introducing the damping constant γ_{coll} and obtain the Lorenzian profile of a damped oscillator with collisions as [13]:

$$I(\omega) = \frac{I_0}{2\pi} \frac{\gamma/2}{(\omega_0 - \omega)^2 + (\gamma/2)^2} \tag{27}$$

where $I_0 = \int I(\omega)d\omega$ and $\gamma = \gamma_n + \gamma_{coll}$. The Kramer's-Kronig relations, when effects of collision is taken into account, become

$$n'_R(\omega) = 1 + \frac{ne^2 f}{4m\varepsilon_0\omega_0} \frac{\omega_0 - \omega}{(\omega_0 - \omega)^2 + (\frac{\gamma}{2})^2} \tag{28}$$

and

$$a(\omega) = \frac{ne^2 f\omega_0}{4m\varepsilon_0 c} \frac{\gamma}{(\omega_0 - \omega)^2 + (\frac{\gamma}{2})^2} \tag{29}$$

In addition to the natural and the pressure broadening there is also Doppler broadening, which is due to the motion of the atoms or molecules of the sample.

Doppler Broadening

The Doppler effect can broaden the absorption line of a vapor medium, which is the consequence of the motion of the atoms of the absorbing medium. The absorption line is broadened by the Doppler effect is inhomogeneous broadening. That is, individual atoms within a collection of identical atoms do not have the same response frequencies since they can have different velocities. The shape associated with the Doppler effect is a Gaussian function. One major contribution

to the spectral line width in gases at low pressures is the Doppler width, which is due to thermal motion of the absorbing or the emitting atoms. Consider an excited atom with a velocity $\vec{u} = (u_x, u_y, u_z)$ relative to the rest frame of the observer. The central frequency of an atomic emission line that is ω_0 in the coordinate system of the atom, is Doppler shifted to $\omega_e = \omega_0 + \vec{k} \bullet \vec{u}$ for an observer looking towards the emitting atom. The apparent emission frequency ω_e is increased if the atom moves towards the observer, and decreased if the atom moves away.

Likewise, one can see that the absorption frequency ω_0 of an atom moving with the velocity $\vec{u}$ across a plane electromagnetic wave $\vec{E}(\vec{x},t) = \vec{E}_0 e^{i(\omega t - \vec{k} \bullet \vec{u})}$ is shifted. The wave frequency ω in the rest frame appears in frame of moving atom as $\omega' = \omega - \vec{k} \bullet \vec{u}$. The atom or molecule can only absorb if ω' that coincide with its resonance frequency ω_0. The absorption frequency $\omega = \omega_a$ is then $\omega_a = \omega_0 + \vec{k} \bullet \vec{u}$. If we choose +z-direction to be the direction of propagation of the wave, we have, with wavevctor $\vec{k} = (0,0,\frac{u_z}{c})$, the absorption frequency ω_a becomes $\omega_a = \omega_0(1 + \frac{u_z}{c})$. At thermal equilibrium the atoms of the gas follow a Maxwellian velocity distribution. At temperature T, the number of atoms or

molecules $h_i(u_z)du_z$ in the level E_i per unit volume with velocity component between u_z and $u_z + du_z$ is [11]

$$h(u_z) = \frac{n_i}{u_p\sqrt{\pi}} e^{-(u_z/u_p)^2} du_z \tag{30}$$

where $n_i = \int h_i(u_z)du_z$ is the atomic number density in the level E_i, $u_p = \sqrt{\frac{2kT}{m}}$ is the most probable velocity, m is mass of the atom and k is the Boltzmann's constant. The number of atoms with absorption frequencies shifted from ω_0 into the interval from ω to $\omega + d\omega$ is [11]

$$h(\omega)d\omega = \frac{n_i}{\omega_0 u_p\sqrt{\pi}} e^{-\left(c\frac{\omega-\omega_0}{\omega_0 u_p}\right)^2} d\omega\,. \tag{31}$$

Since the radiant power emitted or absorbed is proportional to the density of the atoms emitting or absorbing in the interval $d\omega$, the intensity profile of a Doppler broadened spectral line becomes [11]

$$I(\omega) = I_0 e^{-\left(c\frac{\omega-\omega_0}{\omega_0 u_p}\right)^2} \tag{32}$$

This is a Gaussian profile with a half Doppler width $\delta\omega_D = \left(\frac{\omega_0}{c}\right)\sqrt{\frac{2kT\ln 2}{m}} = 3.58\times10^{-7}\bar{\nu}_0\sqrt{\frac{T}{M}}$ in cm^{-1} where T the temperature in Kelvin and M is the mass number. Mostly, both pressure and Doppler broadening effects contribute to the broadening processes at the same time. In such case the line profile becomes the convolution of Gaussian and Lorentzian functions, which gives the Voigt profile.

Voigt Profile

In general, we cannot characterize line shape of a sample as a pure collision broadened Lorentzian or a pure Doppler broadened Gaussian. Both of them may play a role in determining the lineshape. The Voigt profile describes the absorption line shape when both collision and Doppler broadening must be taken into account.

We recall that the special case of Kramer's-Kronig dispersion relation (28) near resonance line is:

$$n'_R(\omega) = 1 + \frac{ne^2 f}{4m\varepsilon_0\omega_0}\frac{\omega_0-\omega}{(\omega_0-\omega)^2+(\frac{\gamma}{2})^2} \qquad (33)$$

To an absorbing atom moving with velocity component $u << c$ away from the source of radiation of frequency ν, the frequency of radiation appears to be shifted, because of Doppler effect, to $\nu' = \nu(1 - \frac{u}{c})$.

Consequently, the real part of the complex index of refraction becomes [11]

$$n'_R(\omega) = 1 + \frac{ne^2 f}{4m\varepsilon_0\omega_0} B(\nu) \tag{34}$$

where $B(\nu)$ is obtained by integrating over the velocity distribution:

$$B(\nu) = \int_{-\infty}^{\infty} \frac{(\nu_0 - \nu + \nu_0 u/c)\sqrt{M/2\pi RT}\, e^{-\frac{Mu^2}{2RT}}}{(\nu_0 - \nu + \nu_0 u/c)^2 + (\delta\nu_L)^2} du .$$

With the parameters x, y, and t where $x = \frac{\nu - \nu_0}{\delta\nu_D}\sqrt{\ln 2}$, $y = \frac{\delta\nu_L}{\delta\nu_D}\sqrt{\ln 2}$, $t = \sqrt{\frac{Mu^2}{2RT}}$, $\delta\nu_L = \frac{\gamma}{4\pi}$ is the Lorentz half width and $\delta\nu_D = \frac{\nu_0}{c}\sqrt{\frac{2RT\ln 2}{M}}$ is the Doppler half width, the function $B(\nu)$ then becomes

$$B(\nu) = -\frac{\sqrt{\ln 2/\pi}}{\delta\nu_D} \int_{-\infty}^{\infty} \frac{(x-t)e^{-t^2}}{(x-t)^2 + y^2} dt = \frac{\sqrt{\ln 2/\pi}}{\delta\nu_D} \mathrm{Im}\left\{ -\frac{i}{\pi} \int_{-\infty}^{\infty} \frac{e^{-t^2}}{(x-t) + iy} dt \right\}$$

$$= \frac{\sqrt{\ln 2/\pi}}{\delta\nu_D} \mathrm{Im}\{w^*(z)\}$$

where $w(z) = \frac{i}{\pi}\int_{-\infty}^{\infty}\frac{e^{-t^2}}{z-t}dt$ [8] and [14]. Thus,

$$n'_R - 1 = \frac{ne^2 f}{16\pi^2 \varepsilon_0 m \nu_0}\frac{\sqrt{\pi \ln 2}}{\delta \nu_D}\mathrm{Im}\{w^*(z)\} \tag{35}$$

Likewise, the absorption coefficient, which is related to the imaginary part of the complex refractive index, is given as [11]

$$a(\nu) = \frac{ne^2 f}{4\varepsilon_0 mc}S(\nu) \tag{36}$$

where the line shape function

$$S(\nu) = \frac{1}{\pi^{3/2}}\frac{y^2}{\delta \nu_L}\int_{-\infty}^{\infty}\frac{e^{-t^2}}{(x-t)^2 + y_2}dt = \frac{1}{\sqrt{\pi}}\frac{y}{\delta \nu_L}\mathrm{Re}\{w(z)\}.$$

Therefore, the absorption coefficient becomes

$$a(\nu) = \frac{ne^2 f}{4m\varepsilon_0 c\sqrt{\pi}}\frac{\sqrt{\ln 2}}{\delta \nu_D}\mathrm{Re}\{w(z)\}. \tag{37}$$

Note that the complex probability function can be written as [8,14] $w(z) = K(x,y) + iL(x,y)$, where $K(x,y)$ and $L(x,y)$ are the real and the

imaginary parts of the complex probability functions respectively. Thus we can rewrite the special cases of Kramer's-Kronig dispersion relations as:

$$n'_R - 1 = -\frac{ne^2 f}{16\pi^{3/2} mc^2 \varepsilon_0 \bar{\nu}_0} \frac{\sqrt{\ln 2}}{\delta \bar{\nu}_D} L(x,y) \tag{38}$$

and

$$a(\bar{\nu}) = \frac{ne^2 f \sqrt{\ln 2}}{4\varepsilon_0 mc^2 \sqrt{\pi} \delta \bar{\nu}_D} K(x,y) = n\sigma(\bar{\nu}) \tag{39}$$

where $\sigma(\bar{\nu}) = \frac{e^2 f \sqrt{\pi \ln 2}}{4\pi\varepsilon_0 mc^2 \delta \bar{\nu}_D} K(x,y)$ is the absorption cross-section for an isolated line [8, 14]. Finally, we can combine the two Kramer's-Kronig relations into one as:

$$n'_R - 1 = \frac{\lambda_0}{4\pi} \frac{\mathrm{Im}\{w^*(z)\}}{\mathrm{Re}\{w(z)\}} a(\bar{\nu}) = n \frac{\lambda_0}{4\pi} \frac{\mathrm{Im}\{w^*(z)\}}{\mathrm{Re}\{w(z)\}} \sigma(\bar{\nu}) \tag{40}$$

This last equation ties the complex index of refraction to the imaginary part and is used to relate the real refractive index of dilute sodium vapor to the frequency.

One can easily see that the above general expression for absorption coefficient, which is the description of the line shape function, reduces to the two independent line functions under the proper limiting cases.

In the Doppler dominated region we have a pure Gaussian function,

$$\lim_{y\to 0} K(x,y) = \lim_{y\to 0} \frac{y}{\pi} \int_{-\infty}^{\infty} \frac{e^{-t^2}}{(x-t)^2 + y^2} dt = \int_{-\infty}^{\infty} \delta(x-t) e^{-t^2} dt = e^{-x^2} \tag{41}$$

Similarly, in a pressure-dominated region, we get

$$\lim_{y\to\infty, x\to\infty} K(x,y) = \lim_{y\to\infty, x\to\infty} \frac{1}{\pi} \int \frac{y e^{-t^2}}{(x-t)^2 + y^2} dt = \frac{1}{\pi} \frac{\delta\bar{\nu}_L}{(\bar{\nu} - \bar{\nu}_0)^2 + (\delta\bar{\nu}_L)^2} \tag{42}$$

which is Lorentzian function.

Chapter 3

OPTICAL MEASUREMENTS

With the optical method, the transmission of the sodium D lines 589.76 nm and 589.16 nm are measured using a discharge sodium lamp as a light source. The sample, which is the sodium metal, is heated with an infrared lamp where the radiated power is controlled with a variac. The temperatures at both ends of the sample holder were measured using thermocouple wires and digital multimeters. When these temperatures stabilize the transmissions were measured using a monochromator that has a resolution of about 0.25 nm at 590 nm. The experimental setup is shown in Figure 1.

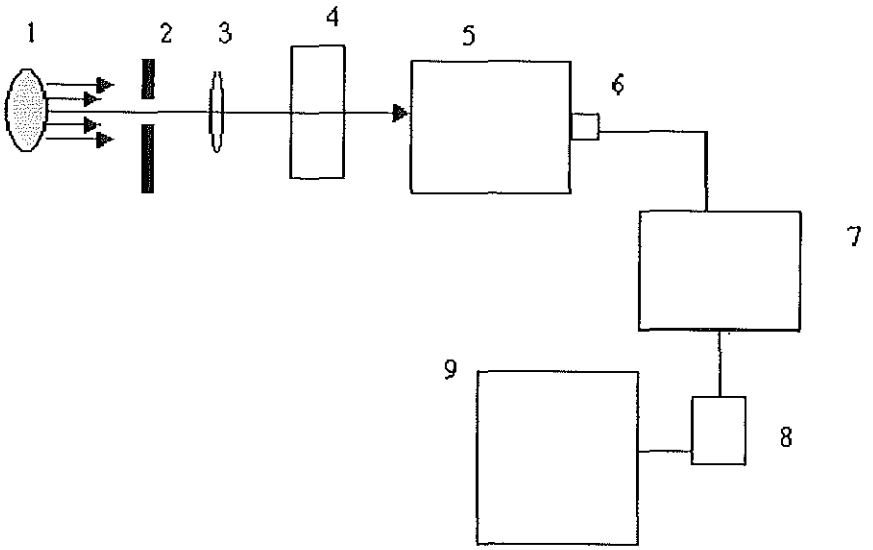

Figure 1 Experimental setup (1) sodium lamp (2) aperture (3) focusing lens (4) sample (5)monochromator (6) detector (7) amplifier (8) multimeter and (9) recorder

Temperature measurements

In order to obtain the temperature of the sample, first, the heat flux per unit area, q, was calculated as [15]

$$q = \frac{T_{colder} - T_{hotter}}{\sum_i R_i} \tag{43}$$

where R_i is the thermal resistance for conduction for each interface. The thermal conductivity of glass at room temperature is 1.4 $\frac{W}{m.K}$ [15] and remains almost constant in the temperature ranges where the measurements were taken. For air the thermal conductivity varies from 26.3×10^{3} $\frac{W}{m.K}$ at 300 K to 43.9×10^{3} $\frac{W}{m.K}$ at 500K. The thermal conductivity of sodium at 473 K is 82 $\frac{W}{m.K}$ and decreases to 76 $\frac{W}{m.K}$ at 573 K. The temperature at each interface is then calculated as [15]

$$T_{i+1} = qR_i + T_i \tag{44}$$

where T_i and T_{i+1} are the temperatures of the adjacent interfaces. The temperature of the sodium vapor was then taken as the average of the temperatures of the glass interfaces, which houses the vapor. The difference of these temperatures also gives the error in the temperature measurements. The temperature distribution for the case when the higher temperature side is 361 K and the lower temperature side is 312 K is shown in Figure 2. The temperature of the vapor in this case is found to be 337 K $\pm$ 1.5 K.

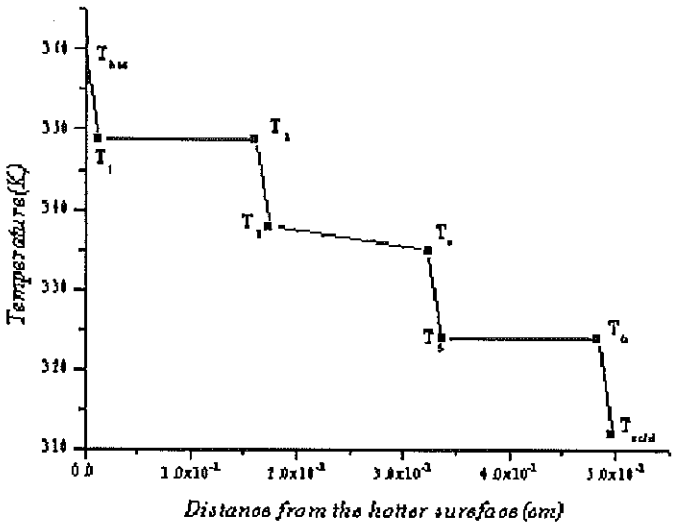

Figure 2 Temperature distribution across the sample housing

Measurement of Transmittance

In the first place, the intensity of the light that the detector receives in the absence of the sodium vapor is measured. The intensity versus the wavelength is plotted with a computer using LABVIEW. At a given temperature of the sample gas, the transmissions were measured three times and each measurement is fitted to a Gaussian profile. The standard deviation is computed to calculate the uncertainty in the intensity measurement. The peak intensity is normalized by the intensity at room temperature, which is 297 K, in order to obtain the transmission. The uncertainty in transmission measurement is computed using the root-mean-square method as:

$$\Delta\tau = \sqrt{\left|\frac{\partial\tau(\nu)}{\partial I_0}\Delta I_0\right|^2 + \left|\frac{\partial\tau(\nu)}{\partial I_t}\Delta I_t\right|^2} \tag{45}$$

where $\tau(\nu)$ is the transmittance at a given temperature, $I_0(\nu)$ is the peak intensity of the incident light, $I_t(\nu)$ is the peak intensity of the transmitted light at the temperature of the measurement, ΔI_0 and ΔI_t are the uncertainties associated with them. The measured transmittances at different temperatures are shown in Figure 5. We see, from these graphs, that the transmittance decreases with as the temperature increases. The maximum error related with the transmittance measurement at 589.76 nm is 1.5 %, while for the 589.16 nm is .08%. In figure 3 the observed intensity at room temperature is shown.

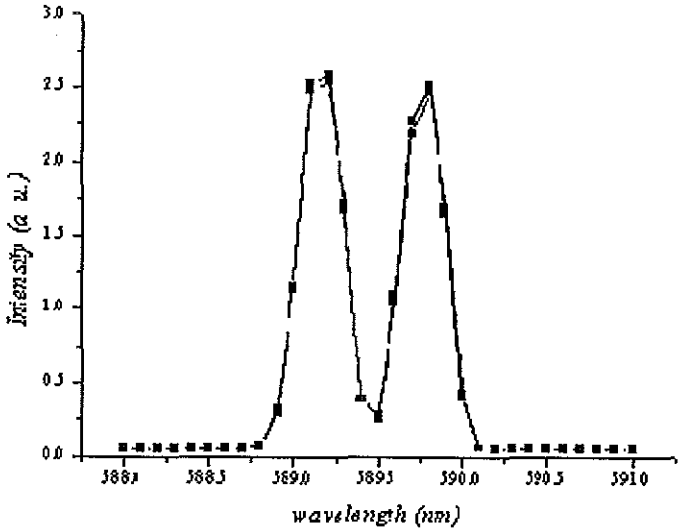

Figure 3 Observed emission lines of tbe Na D transitions at 297 K

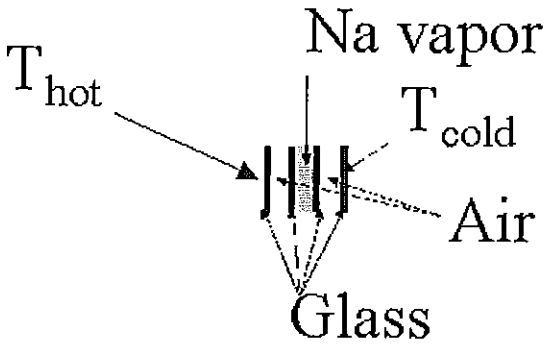

Figure 4 Cross-section of housing for the sample gas

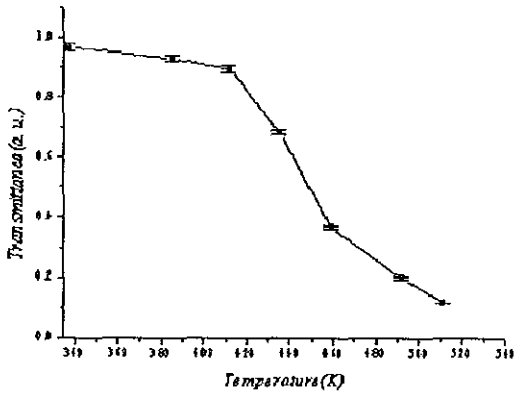

Figure 5 Transmittance as a function of temperature at 589.76 nm

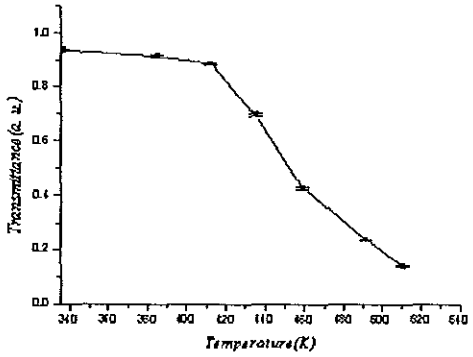

Figure 6 Transmittance as a function of temperature at 589.16 nm

Atomic Number Density

In absorption, the intensity of a transmitted radiation in a gaseous sample medium is given, according to the Beer-Lambert's law [13, 16], as:

$$I_t(\nu) = I_0 e^{-N\sigma(\nu)} \tag{46}$$

where N is the atomic column density and $\sigma(\nu)$ is the absorption cross-section of the sodium atom at the temperature of the measurement. Consequently the transmittance becomes

$$\tau(\nu) = e^{-N\sigma(\nu)} \tag{47}$$

To determine the atomic column density at a particular temperature the absorption on cross-section at the temperature of measurement has to be determined. In general, the absorption cross-section of an isolated i^{th} line is given as [8]:

$$\sigma(\nu) = \sigma_i(\nu) K(x_i, y_i) \tag{48}$$

where $\sigma_i = \dfrac{\sqrt{\pi} r_0 f_i}{\delta \bar{\nu}_D}$ is the integrated absorption cross-section, $\delta \bar{\nu}_D = 3.58 \times 10^{-7} \bar{\nu}_0 \sqrt{\dfrac{T}{M}}$ is the Doppler width in cm^{-1}, $r_0 = 2.8 \times 10^{-13}\ cm$ [11] is classical radius of electron and f_i is the oscillator strength of the i^{th} isolated line, T is temperature in Kelvin, and M is atomic mass number of the sample.

The atomic column density N can be expressed as:

$$N = -\frac{\ln \tau(\nu)}{\sigma(\nu)} \tag{49}$$

Since the transmittances are taken at two different D lines of the sodium atom one can obtain the column density N from the two lines. The two column densities vary slightly. However, by varying the broadening parameters y of the lines the column densities where the minimum difference is attained are taken. At lower temperature, close to room temperature, the values of y lie in the Doppler dominated region. The lower limit for y is the ratio of the natural width to the Doppler width, which is about 0.007. The natural widths of the lines are the lowest possible widths.

The natural width $\delta\bar{\nu}_{ni}$ are related to the associated Einstein coefficients A_i as [11]:

$$\delta\bar{\nu}_{ni} = \frac{A_i}{4\pi c} \tag{50}$$

where c is the speed of light in empty space. From the atomic data [17] the Einstein coefficients are 6.42×10^7 s^{-1} and 6.44×10^7 s^{-1} for 589.76 nm and 589.16 nm sodium lines, respectively.

The absorption cross-section is a function of broadening parameters and the ration of detuning frequency to Doppler with. However, we are interested at resonance frequencies and then the absorption cross-section at resonance becomes a function of only the broadening parameters. That means,

$$\sigma(\nu) = \sigma_i(\nu)K(0, y_i) \tag{51}$$

The difficulty, here, is the determination of the real part of the complex probability function. To simplify this, the complex probability function can be expressed, for y > 0, as [8, 14]

$$w(z) = e^{-z^2}(1 + iErfi(z)) \tag{52}$$

where $Erfi(z)$ is the imaginary error function. On the other hand, the imaginary error function is defined as [4, 5]:

$$Erfi(z) = -iErf(iz) \tag{53}$$

Thus, finally one can see that the complex probability function becomes

$$w(z) = e^{-z^2}(1 + Erf(iz)) \tag{54}$$

The imaginary error function is one of the special functions of *mathematica*™ [8, 19], therefore, $K(0, y)$ can be generated easily and the absorption cross-section at $x = 0$ is computed for different values of y_i. Consequently, the atomic column densities can be obtained using equation 50. However, at a given temperature, the column densities obtained at the two lines must be equal since both of them are column density of the sodium atom. The appropriate values of absorption cross-sections and the corresponding broadening parameters are those, which give minimum difference in column densities. The following procedures were employed in calculating the column densities at various temperatures where the transmission measurements were taken. First at a given temperature the column densities for the lines were calculated for different values of the broadening parameters. Then setting a convergence limit, which is the ratio of the absolute value of the difference of the column densities to their average, the values of the broadening parameters were then varied until minimum ratio is obtained. The appropriate broadening parameters are thus those for which minimum difference attained. The average of the two column densities obtained independently is taken as the column density for that particular temperature of the sodium atom. The difference of the two column densities set the error limit for the column density. From the plot of the transmittance versus the column density the transmission is observed to decrease as shown in figure 7. The transmittance is a measured quantity and absorption cross-section is calculated using the Voigt

profile. As shown in figure 6 the peak absorption cross-section decreases exponentially as the broadening parameter y increases.

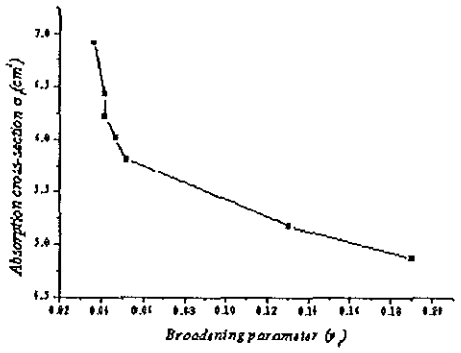

Figure 7 Variation of peak absorption cross-section with broadening parameter at 589.76 nm

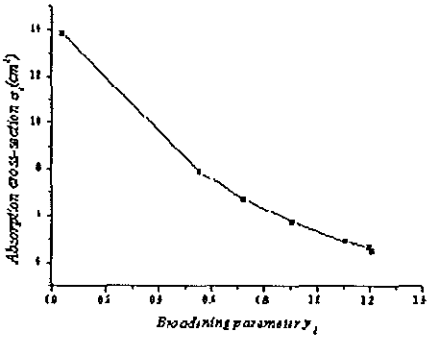

Figure 8 Peak absorption cross-section as a function of broadening parameter y at 589.16 nm

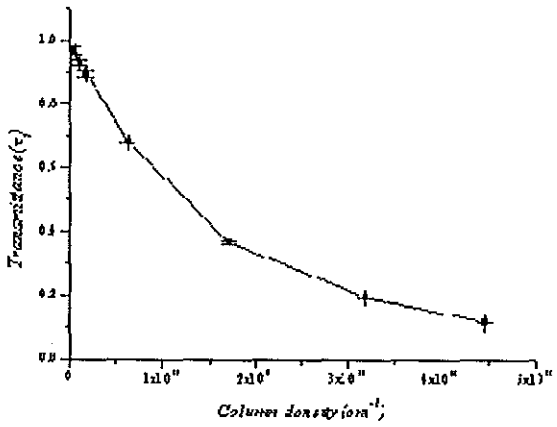

Figure 9 Transmittance as a function of column density at 589.76 nm

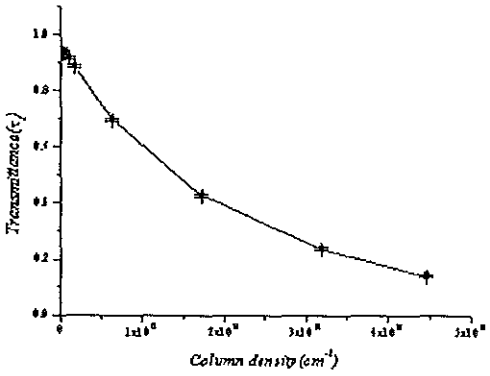

Figure 10 Transmittance versus column density at 589.17 nm

Once the column densities at different temperatures are determined, it is easy to obtain the corresponding atomic number density. The number density is the ratio of the column density to the path length in the sodium vapor. The path length l is 2.98 ± 0.01 cm. Thus, the number density at a given temperature is $n = \frac{N}{l}$. The uncertainty in number density n, making use of the root-sum-square method, is given as

$$\Delta n = \sqrt{\left|\frac{\partial n}{\partial N}\Delta N\right|^2 + \left|\frac{\partial n}{\partial l}\Delta l\right|^2} \tag{55}$$

The number densities n at different temperatures T is plotted in figure 11. The atomic number density increases exponentially as the temperature increases.

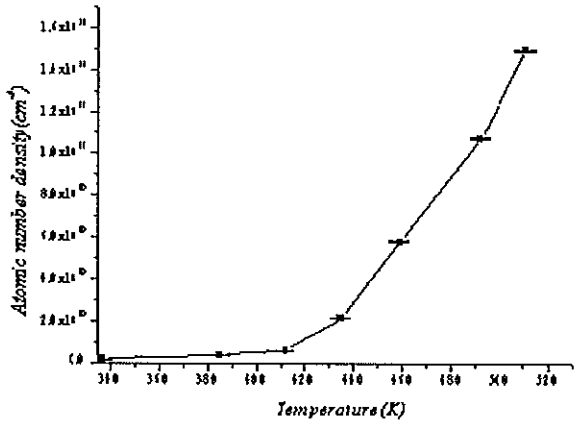

Figure 11 number densities as function of temperature

Absorption coefficient and index of refraction at the sodium D Lines

Making use of the number densities and the broadening parameters discussed in the previous section, it is possible to plot the absorption coefficient $a(\bar{\nu}) = n\sigma(\nu)$ versus wavenumber $\bar{\nu}$ as shown in figures below.

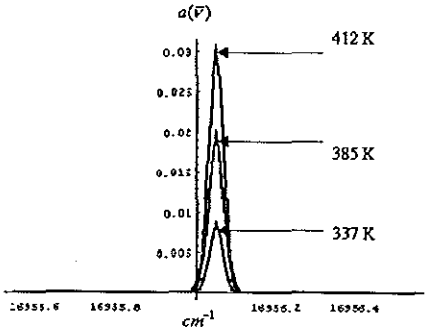

Figure 12 Absorption coefficients in cm^{-1} at 589.76 nm for temperatures 337 K, 385 K, 412 K

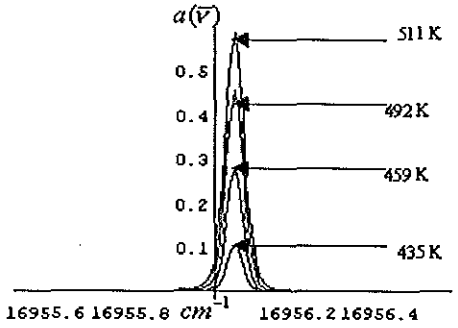

Figure 13 Absorption coefficients in cm^{-1} at 589.76 for temperatures 435 K, 459 K, 492 K, 511 K

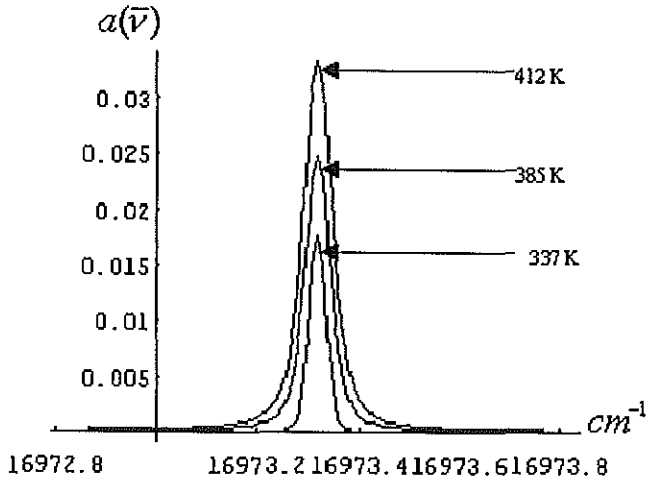

Figure 14 Absorption coefficient in cm^{-1} at 589.16 nm for temperatures 337 K, 385 K, and 412 K

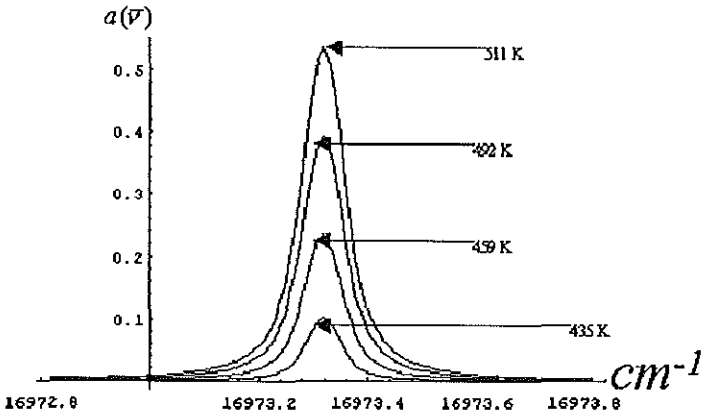

Figure 15 Absorption coefficients in cm^{-1} at 589.16 nm for temperatures 435 K, 459 K, 492 K, and 511 K

With the knowledge of atomic number density and the broadening parameters, the real part of the complex index of refraction for the two D lines in the temperature ranges the transmission measurements taken are plotted.

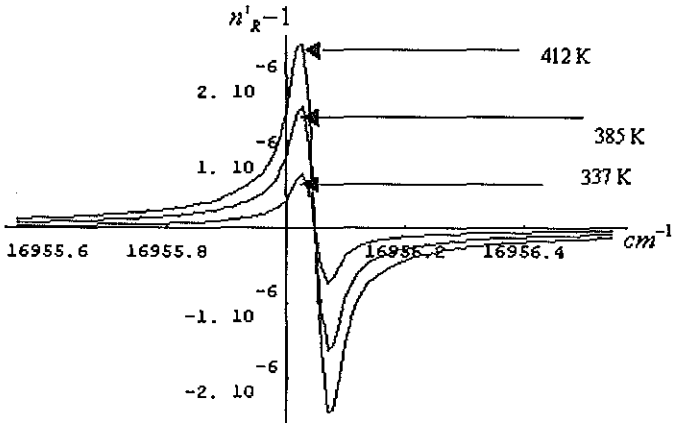

Figure 16 Index of refraction at 589.76 nm for temperatures 337 K., 385 K, and 412 K

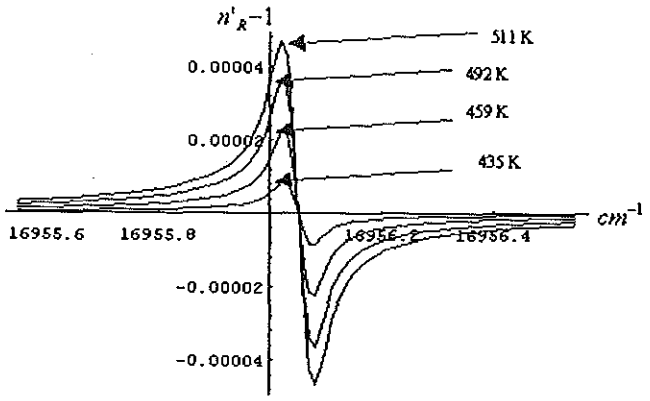

Figure 17 Index of refraction at 589.76 nm for temperatures 435 K., 459 K, 492 K, and 511 K

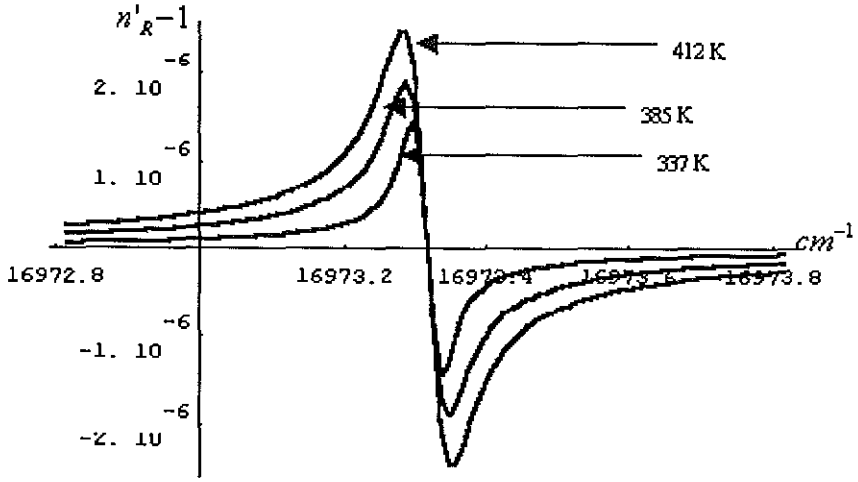

Figure 18 Index of refraction at 589.16 nm for temperatures 337 K., 385 K, and 412 K

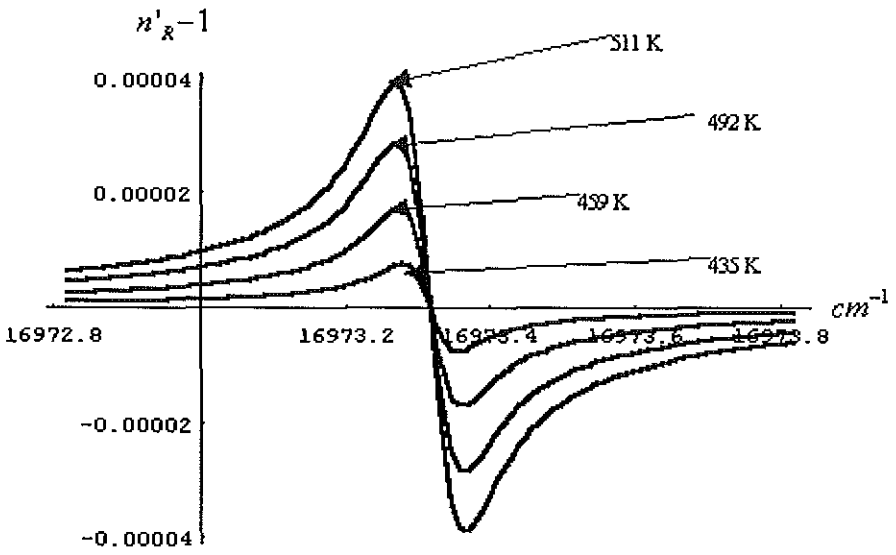

Figure 19 Index of refraction at 589.16 nm for temperatures 435 K., 459 K, 492 K, and 511 K

As one can observe from the graphs plotted above, normal dispersion is observed at far off resonance. On the other hand, in the region near to resonance line a different violent behavior is observed. Such dispersion processes are said to be anomalous dispersion. In this last case the real index of refraction decreases as the frequency decreases. Moreover, it is observed that away from resonance region the real index of refraction increases with increase in number density.

Determination of vapor pressure

In the temperature ranges of interest the atomic number density is relatively small since the vapor is dilute. Consequently, we can consider the vapor as an ideal gas.

Thus applying the ideal gas law, one obtains the relation, at vapor pressure p, temperature T, and number density n, [2]

$$p = \left(\frac{p_0}{n_0 T_0} \right) nT \tag{56}$$

where T_0 and p_0 are the standard temperature and pressure (STP) and $n_0 = 2.6873 \times 10^{19}$ cm^{-3} [20] is the Loschmidt number (Loschmidt number is number of atoms or molecules per unit volume of an ideal gas at 273.15 K and normal atmospheric pressure (760 Torr) [20]). The values of vapor pressure of sodium at different temperatures, as shown in figure 20, vary from 76 $nTorr$ at 337 K to 8 $\mu Torr$ at 511 K.

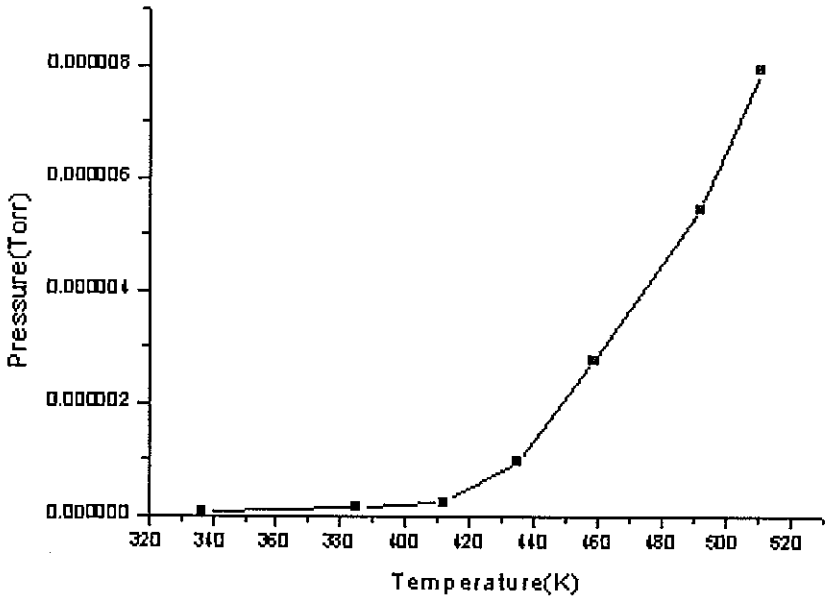

Figure 20 Pressure distribution as a function temperature of sodium atomic vapor

From the broadening parameters obtained it is possible to estimate the natural lifetime of an excited sodium atom. As the mathematical derivation is given in detail in [13] the total transition probability for the depopulation of an excitation level is a sum of radiative and collision-induced transition probabilities [13]:

$$A_i = A_{rad} + A_i^{coll} \tag{57}$$

where $A_i^{coll} = n\sigma_i u$, n and u have the same meaning as in the previous sections, and σ_i is the imaginary part of the quenching cross-section. Using the

thermodynamic equation of state $p = nKT$ the number density n can be expressed in terms of pressure p. In addition, since the radiative transition probability A_{rad} can be expressed as radiative lifetime τ_{sp} as:

$$A_{rad} = \frac{1}{\tau_{sp}} \tag{58}$$

Therefore, the total transition probability can be rewritten as

$$A_{rad} = \frac{1}{\tau_{sp}} + ap \tag{59}$$

where $a = 4\sigma_i \sqrt{\frac{1}{mKT}}$. This is the Stern-Vollmer equation, and is helpful to determine the radiative lifetime of an excited atom. In order to get the lifetime the total transition probability versus the vapor pressure is plotted. The value at which the vapor pressure is 0 (the intercept of A_i) gives us the desired natural lifetime. The total transition probability is obtained from the relation $A_i = 2\pi y \delta \bar{v}_D$. Making use of linear fit analysis the radiative lifetime of sodium is found to be about4 *ns*.

Figures 21 and 22 shows the total transition probability versus the vapor pressure at 589.76 nm of sodium.

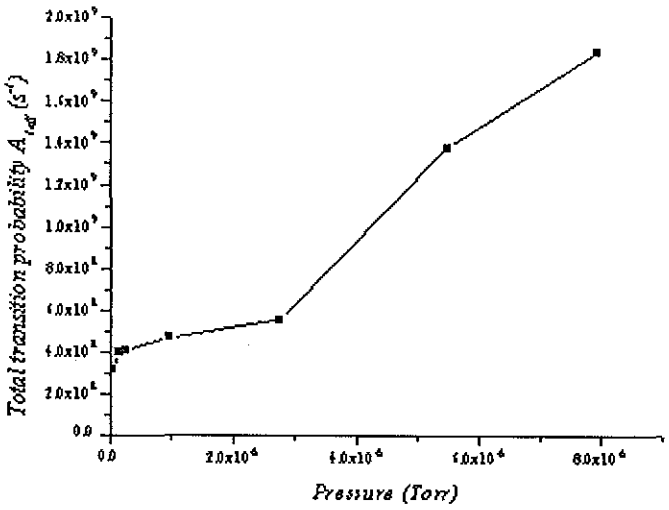

Figure 21 Transition probability versus pressure at 589.76 nm

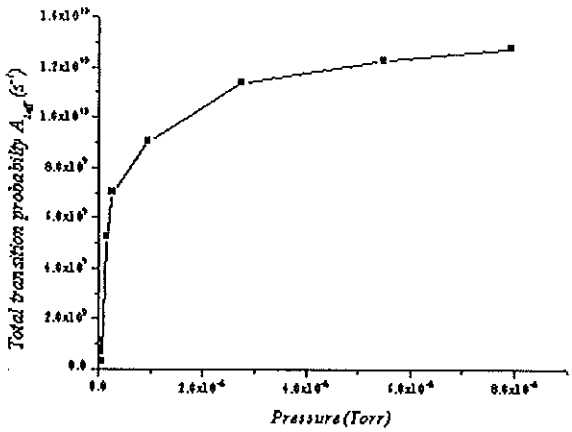

Figure 22 Transition probability versus pressure at 589.16 nm

Chapter 4

CONCLUSION

The most important results of the experiment are the following. The vapor pressure of sodium atom has been incomplete since the data available were for higher temperatures. The vapor pressure obtained in this thesis completes the curve. The broadening parameters, absorption coefficient and index of refraction are important atomic data for verification of theories. Therefore, these determined values would provide important information for atomic physics.

Making use of the two D lines, number density of sodium atom is determined. In addition, since the vapor is diluted, applying equation of state, the vapor pressure of sodium atom at lower in the temperature ranges from 337 K to 511 K found to vary from 76 *nTorr* to 8 *μTorr* . This is an important method to determine the partial vapor pressure of a particular gas when a sample is a mixture of atoms of different species.

The peak absorption coefficient $a(\bar{\nu})$ varies from 0.02 cm^{-1} at 337 K to 0.6 cm^{-1} at 511 K for 589.16 nm and 0.01 cm^{-1} at 337 K to 0.7 cm^{-1} at 511 K for 589.76 nm. in the range from 337 K to 511 K, the number density varies from 10^9 cm^{-3}

at 337 K to 10^{12} cm^{-3}. Moreover, as the temperature increases or the number density increase the region of anomalous dispersion increases for both D lines of sodium atom.

The lifetime of sodium atom determined at low pressure is less than that determined at higher temperatures. In this experiment, which is done for low pressure of Na, the atomic natural lifetime of an excited Na atom is about 4 *ns*.

Bibliography

1. Ditchburn R. W. and Opik V., Atomic and molecular processes, edited by Bates D. R., Academic presses Inc., New York, 1962

2. Hudson D., Phys. Rev. A, 135, A1212 (1964)

3. Bjorkholm E. and Ashkin A., Phys. Rev. Let. 32, 129 (1974)

4. JANAF Thermo chemical Tables, The Dow chemical company, Midland, Michigan, 1962

5. Hultgren R., Orr R. L., Anderson P. D. and Kelley K. K., selected values of thermodynamic properties of metals and alloys, John Wiley and Sons, Inc., New York, 1963

6. Honig R. E. RCA Rev. 23, 567 (1962)

7. Nesmeyanov A. N., Vapor pressure of chemical elements, edited by Robert Gary, Elsevier Publishing Co., Inc., New York, 1963

8. Asfaw A., JQSRT, 70, 2, (2001)

9. Suter D., The physics of Laser-Atom Interaction, Cambridge University Press, New York, 1997

10. Corney A., Atomic and Laser Spectroscopy, Oxford University Presses, 1986

11. Milonni W. P. and Eberly H. J. Lasers, John Wiley and Sons, inc., New York, 1988

12. Jackson J. D., Classical electrodynamics, 2nd edition, John Wiley and Sons, New York, 1975

13. Demtroder, Laser Spectroscopy: Basic concepts and instrumentation, 2nd edition, Springer-Verlag Berlin Heidberg, 1996

14. Armsrong B. H., JQSRT 7, 61 (1967)

15. Incorpera F. P., and Dewitt D. P., Fundamentals of heat transfer, John Wiley and Sons, Inc., New York, 1981

16. Thorne A. P., Spectrophysics, 2nd edition, English Language Book Society/ Chapman and Hall Ltd, 1988

17. NIST Atomic Database, (WWW.NIST.GOV)

18. Young C., JQSRT 5, 549 (1986)

19. Stephen Wolfram, Mathematica: A system for doing mathematics by computer, 2nd edition, Addison-Wesley publishing company Inc.,Red Wood City, California, 1991

20. Lide D. R., Handbook of chemistry and physics, 70th edition, CRC presses Inc., 1990

21. Hercke B., App. Phys. A, 40, 151 (1986)

22. Zaidel A.N., and Shreider E. Ya., Vacuum Ultraviolet Spectroscopy, Translated by Lerman Z., Israel Program for Scientific Translations, Halsted Press, John Wiley and Sons, Inc., New York, 1970

23. Ditchburn, Light, 3rd edition, Academic press, New York, 1976